# Ipsilateral cortical fMRI responses after peripheral nerve damage in rats reflect increased interneuron activity

Galit Pelled[a,1,2], Debra A. Bergstrom[b], Patrick L. Tierney[c], Richard S. Conroy[a], Kai-Hsiang Chuang[a], David Yu[d], David A. Leopold[e], Judith R. Walters[b], and Alan P. Koretsky[a]

[a]Laboratory of Functional and Molecular Imaging and [b]Neurophysiological Pharmacology Section, National Institute of Neurological Disorders and Stroke, National Institutes of Health, Bethesda, MD 20892; [c]McGovern Institute for Brain Research, Massachusetts Institute of Technology, Cambridge, MA 02139; [d]Laboratory of Neuropsychology, National Institute of Mental Health, National Institutes of Health, Bethesda, MD 20892; and [e]Unit on Cognitive Neurophysiology and Imaging, Laboratory of Neuropsychology, National Institute of Mental Health, National Institute of Neurological Disorders and Stroke, National Eye Institute, National Institutes of Health, Bethesda, MD 20892

Edited by Leslie G. Ungerleider, National Institutes of Health, Bethesda, MD, and approved July 7, 2009 (received for review March 21, 2009)

**In the weeks following unilateral peripheral nerve injury, the deprived primary somatosensory cortex (SI) responds to stimulation of the ipsilateral intact limb as demonstrated by functional magnetic resonance imaging (fMRI) responses. The neuronal basis of these responses was studied by using high-resolution fMRI, in vivo electrophysiological recordings, and juxtacellular neuronal labeling in rats that underwent an excision of the forepaw radial, median, and ulnar nerves. These nerves were exposed but not severed in control rats. Significant bilateral increases of fMRI responses in SI were observed in denervated rats. In the healthy SI of the denervated rats, increases in fMRI responses were concordant with increases in local field potential (LFP) amplitude and an increased incidence of single units responding compared with control rats. In contrast, in the deprived SI, increases in fMRI responses were associated with a minimal change in LFP amplitude but with increased incidence of single units responding. Based on action potential duration, juxtacellular labeling, and immunostaining results, neurons responding to intact forepaw stimulation in the deprived cortex were identified as interneurons. These results suggest that the increases in fMRI responses in the deprived cortex reflect increased interneuron activity.**

imaging | plasticity | somatosensory cortex | nerve injury | cortical interneurons

Functional magnetic resonance imaging (fMRI) techniques permit the longitudinal monitoring of the brain's reorganization after central and peripheral injury. Increased fMRI responses in inappropriate areas of the somatosensory cortex that are not normally activated in response to stimuli have been observed in stroke, multiple sclerosis, and limb-amputation patients (1–3). In rats, stimulation of a limb results in fMRI responses mainly in the contralateral primary somatosensory cortex (SI) (4, 5). However, 2 weeks after complete denervation of the rat's limb, sensory stimulation of the intact forepaw induces fMRI responses in both the contralateral (healthy) and the ipsilateral (deprived) SI (6). Ablating the healthy SI representation ipsilateral to the denervated limb eliminates the fMRI responses in the deprived cortex, suggesting that increases in the fMRI responses in the ipsilateral SI are principally mediated through interhemispheric communication (6).

It is generally acknowledged that increases in blood oxygenation level-dependent (BOLD) fMRI responses represent increased neuronal activity (7), and decreases in BOLD responses represent decreased neuronal activity (8–10) as reflected in local field potentials (LFP). However, the exact relationship between the neuronal activity of specific classes of neurons and the vascular response leading to BOLD signals is still not understood. For example, in addition to pyramidal neurons and glial cells releasing vasodilators, increases in inhibitory interneuron activity can enhance blood flow in the cerebellum (11) and induce vessel vasodilation (12, 13). Furthermore, increased BOLD responses in monkey SI have been attributed to net local inhibition (14). Thus, it is unclear how the fMRI responses observed in inappropriate cortical areas of human patients and rodents should be interpreted after plasticity following recovery from central or peripheral nerve injury.

In the present work, data from high-resolution fMRI, in vivo electrophysiological recordings, and juxtacellular neuronal labeling techniques were obtained to gain insight into the neuronal basis of the bilateral fMRI responses in the rodent SI after unilateral peripheral nerve injury. After limb denervation, the increased fMRI responses within the deprived SI that are elicited by stimulation of the intact forepaw are associated primarily with increased activity of interneurons with minimal changes in LFP.

## Results

**Functional MRI.** Effects of forepaw stimulation on cortical activity were examined in rats with permanent denervation of the right forepaw and in sham-operated controls. BOLD fMRI was carried out at 11.7 T, permitting high spatial ($150 \times 150 \times 1{,}000$ $\mu$m) and excellent temporal (750 ms) resolution. Fig. 1*A* shows high-resolution fMRI group $t$ test maps ($n = 7$) of sham-operated and denervated rats overlaid on echo-planar MRI images [bregma −0.3 mm according to Paxinos and Watson (15)] obtained 2–3 weeks after surgery. In agreement with previous work (6), when the intact forepaw of the denervated rat was stimulated, both contralateral healthy and ipsilateral deprived SI exhibited significant fMRI activation: 153 ± 32 pixels were activated in the healthy SI cortex and 55 ± 13 pixels in the deprived SI cortex (ANOVA, $F = 11.088$, $P < 0.001$, post hoc Student Newman Keuls comparison $P < 0.05$). Moreover, the magnitudes of these mean fMRI responses were greater in the denervated rats in both the contralateral healthy (5.0 ± 0.8% BOLD signal change) and the ipsilateral deprived (1.8 ± 0.3%) SI, compared with the SI responses in sham-operated rats (3.3 ± 0.3% and 0.4 ± 0.2%, respectively) (ANOVA $F = 18.182$, $P < 0.001$, post hoc Student Newman Keuls, all comparisons $P < 0.05$).

Author contributions: G.P., D.A.B., D.A.L., J.R.W., and A.P.K. designed research; G.P., D.A.B., P.L.T., R.S.C., D.Y., J.R.W., and A.P.K. performed research; G.P., D.A.B., R.S.C., K.-H.C., J.R.W., and A.P.K. analyzed data; and G.P., D.A.B., D.A.L., J.R.W., and A.P.K. wrote the paper.

The authors declare no conflict of interest.

This article is a PNAS Direct Submission.

Freely available online through the PNAS open access option.

[1]Present address: Kennedy Krieger Institute and Radiology Department, Johns Hopkins School of Medicine, Baltimore, MD 21205.

[2]To whom correspondence should be sent at the present address. E-mail: pelled@kennedykrieger.org.

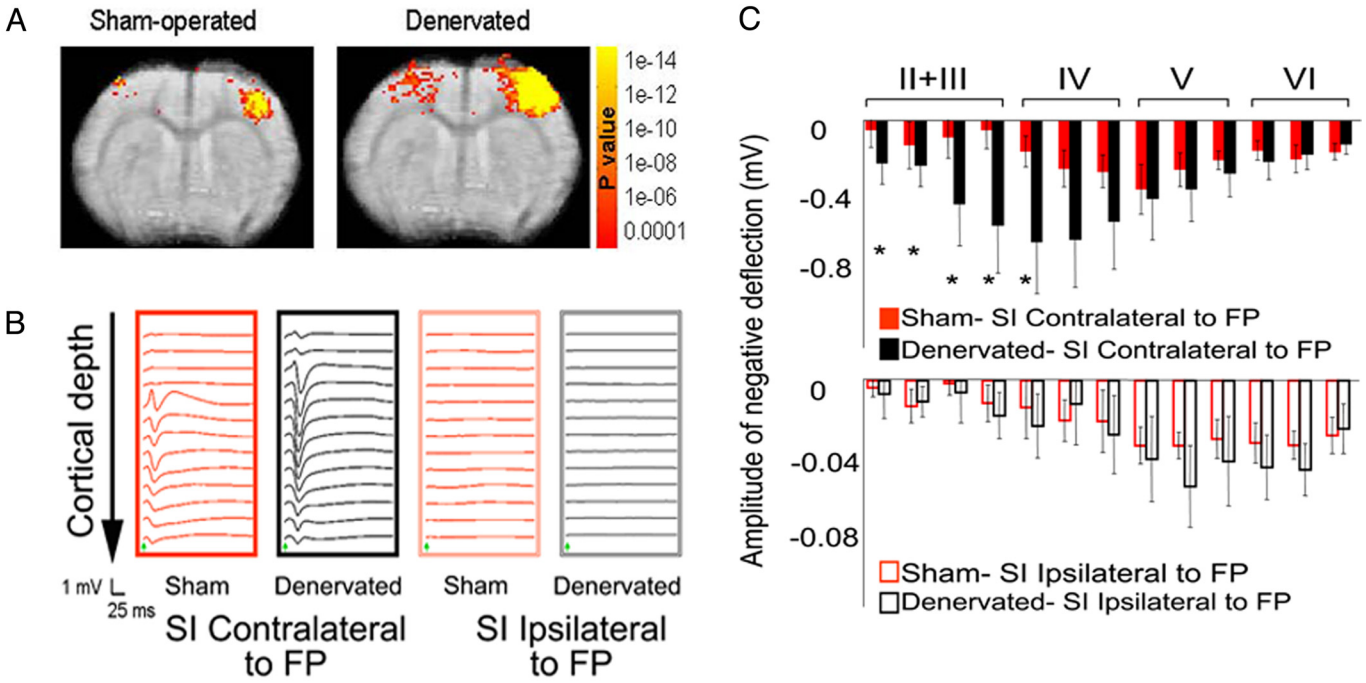


**Fig. 1.** fMRI and LFP responses to forepaw stimulation in the SI of sham-operated and denervated rats. (*A*) Group averaged functional MRI *t* test maps overlaid on echo-planar MRI of SI activation after forepaw stimulation in sham-operated and denervated rats. In sham-operated rats ($n = 7$), stimulation of a forepaw resulted in significant contralateral SI activation with minimal ipsilateral SI activation. In contrast, when the healthy forepaw was stimulated in denervated rats ($n = 7$), both contralateral and ipsilateral SI exhibited significantly larger fMRI activation area. The number of pixels above the cross-correlation threshold was calculated for each individual rat and averaged across the group. Because the forepaw representation is slightly different for each individual rat, these averaged *t* test maps may not precisely define SI representation. (*B*) Stimulus-induced LFP responses in individual rats, beginning 50 $\mu$m below the SI cortical surface with LFP recordings performed at 150-$\mu$m increments. Marked changes in LFP activity were observed when the forepaw (FP) contralateral to the recorded SI was stimulated in sham-operated and denervated rats. However, stimulation of the forepaw ipsilateral to the recorded SI resulted in minimal change in LFP activity in either group. Green arrows indicate stimulus onset. (*C*) Group averages of stimulus-induced LFP negative deflection amplitude. The amplitude of the initial negative deflection of the LFP response in the denervated rats was greater in the healthy cortex, in particular in lamina IV, when the intact forepaw was stimulated. Significant differences were also observed in lamina II + III. However, the amplitudes of the LFP deflection in both control and denervated rats were similar in the SI cortex ipsilateral to the forepaw stimulation. Note the 10-fold scale difference between responses to contralateral (*Upper*) and ipsilateral (*Lower*) stimulation (*, paired *t* test, $P < 0.05$).

**LFP Recordings.** Measurements of both the spontaneously active and stimulus-induced spiking of individual neurons, along with the LFP responses at multiple equally spaced cortical depths ranging from 50 to 1,850 $\mu$m below the pia mater were assessed. The response pattern was generally similar for the two groups in that stimulation of the contralateral forepaw elicited LFP responses that were an order of magnitude greater than stimulation of the ipsilateral forepaw (Fig. 1*B*). However, quantitative analysis of the LFP peak negative deflection, thought to reflect both thalamocortical and corticocortical inputs, revealed significantly greater responses in the superficial laminae (between 50- and 800-$\mu$m depth) of the denervated rats compared with controls (paired Student *t* test, $P < 0.05$) after stimulation of the contralateral forepaw (Fig. 1*C Upper*). The mean latency of the peak negative deflection of the LFP response across the cortical laminae was similar in both groups (12 ± 5 ms and 13 ± 3 ms, respectively). Importantly, there were no significant differences in the magnitude of LFP responses to ipsilateral forepaw stimulation between the two groups (Fig. 1*C Lower*).

**Single-Unit Recordings.** Given the apparent discrepancy in the ipsilateral responsiveness of the BOLD and LFP signals, the responsiveness of isolated single neurons to stimulation was investigated. All well-isolated spontaneously active neurons encountered as recording electrodes were slowly advanced through the cortex were tested for response to contralateral and/or ipsilateral forepaw stimulation. A total of 177 neurons from 12 rats (6 sham-operated and 6 denervated) were isolated. Increases in spiking in response to ipsilateral forepaw stimulation were examined. No neurons were found that responded to ipsilateral stimulation in sham-operated rats [0 of 60 neurons (0%)]. However, in the denervated rats, 21% of the neurons responded to ipsilateral stimulation (13 of 62; $\chi^2 = 11.965$, $P < 0.001$). Interestingly, these responsive neurons were found in the infragranular laminae V and VI. Thus, the evoked ipsilateral spiking responses differed markedly between the two groups. Although there was no significant difference in ipsilateral stimulus-triggered LFP responses, a significant number of responsive neurons could be found in the denervated cortex.

Increases in spiking in response to contralateral stimulation were also significantly affected by denervation. In the denervated group, significantly more neurons responded to the stimulus [30 of 55 (55%)] compared with controls [18 of 60 (30%); $\chi^2 = 6.136$, $P = 0.013$]. Increases in spiking activity responses in the healthy cortex of denervated rats were found in all cortical laminae except lamina I. Representative poststimulus time histograms are shown in Fig. 2.

Because of the discrepancy between the lack of LFP response and the increased single-neuron and fMRI responses in the deprived cortex, it was hypothesized that responses to ipsilateral forepaw stimulation might reflect increased responsiveness of a population of inhibitory interneurons. Interneurons constitute ≈20% of all cortical neurons and are thought to make a small contribution to the LFP but have the potential to influence neurovasculature coupling (12, 13). One means of characterizing neurons is by the width of their action potentials (AP). It has previously been demonstrated that the APs of interneurons in

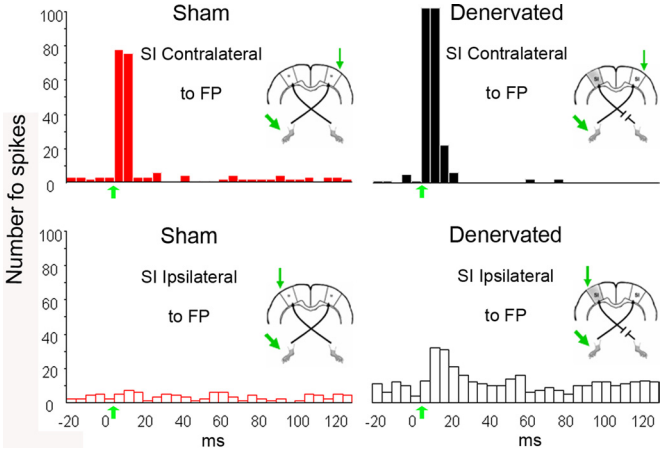


**Fig. 2.** Poststimulus time histograms illustrating spiking responses to forepaw stimulation. In sham-operated rats, contralateral, but not ipsilateral, stimulation of the forepaw (FP) resulted in increased neuronal spiking. In denervated rats, stimulation of the intact forepaw resulted in increased neuronal spiking in both contralateral (healthy) and ipsilateral (deprived) cortices. Green arrows on time axis represent stimulus onset. Diagrams represent site of cortical recordings and forepaw stimulations.

the cerebral cortex have secondary phases that are shorter than those of pyramidal neurons (16). Fig. 3*A* illustrates traces of APs from two groups of neurons: one set exhibiting longer AP durations and another set exhibiting shorter AP durations. Most neurons [11 of 13 (85%)] that increased their spiking in response to ipsilateral stimulation in the deprived cortex had AP durations <0.5 ms, consistent with AP characteristics of interneurons. The averaged AP duration of these neurons was 0.36 ± 0.03 ms. In contrast, most neurons [31 of 48 (65%)] responsive to contralateral stimulation in controls and in the healthy cortex of the denervated rats exhibited AP durations >0.5 ms, consistent with

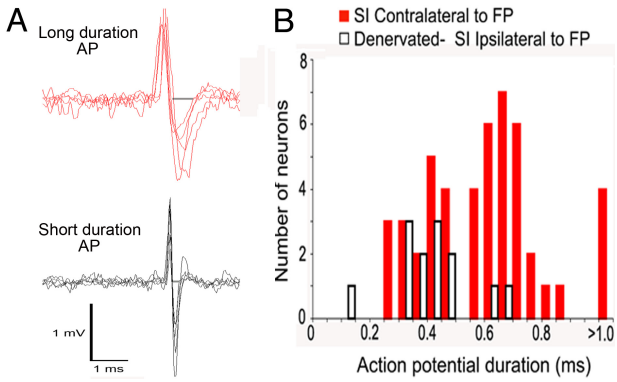


**Fig. 3.** Examples of extracellular AP waveforms for putative pyramidal neurons and interneurons and distribution of AP durations of neurons that responded to forepaw stimulation. (*A*) AP waveforms of 5 long-AP-duration neurons (putative pyramidal neurons) and 5 short-AP-duration neurons (putative interneurons). The segments used for measurement of AP duration are indicated by the gray bars. (*B*) Interneurons in the cerebral cortex typically have shorter AP durations compared with pyramidal neurons. Therefore, we measured the AP duration of the neurons that responded to forepaw stimulation. All neurons that responded to contralateral forepaw stimulation with increases in firing rate in sham-operated or denervated rats are shown with their corresponding AP duration (red bars). The majority of neurons (31 of 48) that responded to contralateral stimulation with increases in firing rate in sham-operated or denervated rats had AP durations >0.5 ms. However, most neurons (11 of 13) that responded to ipsilateral forepaw stimulation in the deprived SI in denervated rats had AP durations < 0.5 ms (black-outlined bars).

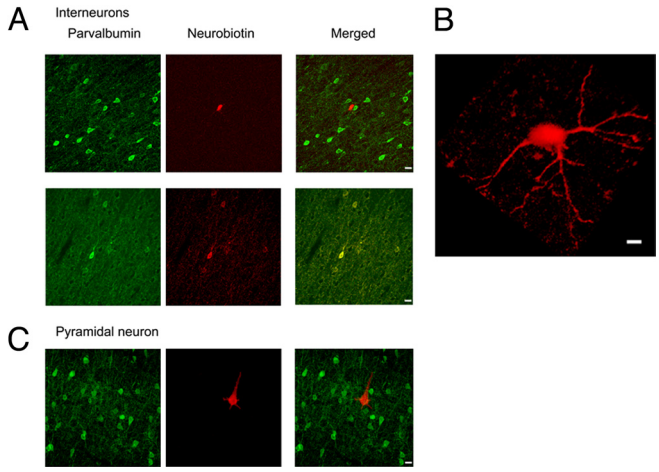


**Fig. 4.** Juxtacellular labeling of neurons in the deprived somatosensory cortex of the denervated rats. (*A*) Two examples of in vivo juxtacellular neurobiotin-labeled neurons in lamina V within the deprived SI. Interneurons were identified by their cell size and gross morphology. Both parvalbumin positive and negative interneurons were identified. These neurons responded to stimulation of the (ipsilateral) intact forepaw. (Scale bars, 10 $\mu$m.) (*B*) A 3D reconstruction of an individual neurobiotin-labeled neuron showing characteristic morphology of an interneuron. (*C*) A pyramidal cell within the deprived SI cortex that did not respond to ipsilateral forepaw stimulation.

AP characteristics of pyramidal neurons. The averaged AP duration of these neurons was 0.70 ± 0.02 ms (Student *t* test, $P < 0.001$, $t = 8.928$). Fig. 3*B* shows the distribution of AP durations of neurons that responded to contralateral (red bars) or ipsilateral (open black bars) forepaw stimulation.

**Juxtacellular Labeling.** To further characterize the neuronal population responding to ipsilateral stimulation after denervation, in vivo juxtacellular labeling (16) and extracellular recordings were performed in another group of 12 denervated rats. An additional 86 neurons were recorded; 14 neurons increased spiking in response to ipsilateral stimulation. AP duration analysis identified 13 of 14 neurons as interneurons. Twelve of these interneurons were successfully labeled with neurobiotin. Cell size (11.6 ± 2.6 $\mu$m) and gross morphology were consistent with all 12 neurons being interneurons as compared with parvalbumin-stained interneurons, This corroborates and strengthens the AP findings presented above. Two examples of neurobiotin-labeled cells are shown in Fig. 4 *A* and *B*. An additional 2 neurons that did not demonstrate increased spiking in response to stimulation had morphology consistent with pyramidal neurons (cell size 25.8 ± 1.6 $\mu$m, Fig. 4*C*).

**Pyramidal Neuronal Activity.** Pyramidal neurons (as defined by long-duration APs) located in laminae V and VI of the ipsilateral SI did not show a rapid, time-locked increase in spiking in response to stimulation. These were characterized with respect to the more prolonged effects of ipsilateral forepaw stimulation on firing rate. In sham-operated rats, 2 of 45 (4%) pyramidal neurons showed mean decreases in firing rate (>10%) during the period of ipsilateral forepaw stimulation. In contrast, significantly more pyramidal neurons, 18 of 98 (18%; $\chi^2 = 4.969$, $P < 0.05$), in the deprived cortex of denervated rats showed firing rate decreases during the stimulation period (Fig. 5). A pyramidal neuron response to ipsilateral stimulation is shown in Fig. 5*A*. The overall mean inhibition during stimulation was 36.5 ± 4.7% ($n = 18$), a significant decrease in firing rate compared with prestimulation baseline (paired *t* test, $t = 6.431$, $P < 0.0001$, Fig. 5*B*). In 11 of 18 of the pyramidal neurons, the stimulus-induced

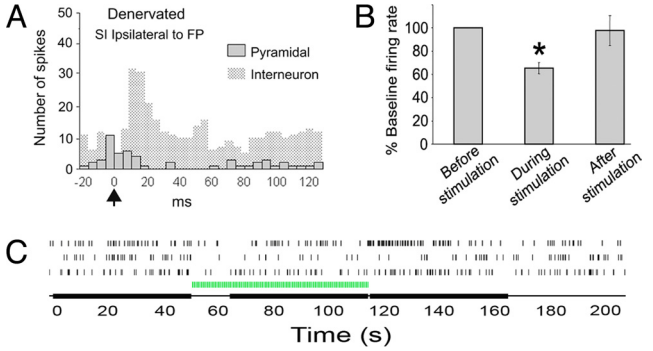


**Fig. 5.** Spiking responses of putative pyramidal neurons in the deprived cortex to forepaw (FP) stimulation. (*A*) Poststimulus time histogram illustrating spiking responses to intact ipsilateral forepaw stimulation of a pyramidal (dotted bars) and an interneuron (solid gray bars) located in the deprived cortex of the denervated rat. The histogram of the spiking response of an interneuron to ipsilateral stimulation (also shown in Fig. 2) is superimposed on the histogram of a pyramidal neuron response to illustrate differences in the timing responses of these 2 neuronal populations. (*B*) Eighteen neurons in the deprived cortex that did not respond to ipsilateral forepaw stimulation were identified as pyramidal neurons according to their AP duration. During ipsilateral forepaw stimulation, these neurons decreased their firing rate by 36.5 ± 4.7% and returned to baseline during the 50-s poststimulation (*, paired *t* test, $P < 0.001$). (*C*) Three spike trains obtained from three pyramidal neurons (identified according to their AP duration) in the deprived cortex showing decreased firing rate during stimulation of the intact ipsilateral forepaw. Green bar represents stimulation epoch; black bars represent time epochs selected for calculations. Rebound excitation is clearly demonstrated in the top trace.

inhibition was followed by rebound excitation (firing rate increased >10% compared with baseline firing rate; see Fig. 5*C*, top trace) after termination of stimulation. The timing of this effect was variable, and the population response during the post stimulation period was not significantly different from baseline. The decrease in firing rate of pyramidal neurons during stimulation is consistent with increased inhibition due to increased interneuron firing in the ipsilateral, deprived cortex.

## Discussion

This study demonstrates significant bilateral increases in fMRI responses in the SI after sensory deprivation. The greater amplitude and spatial extent of the fMRI responses are associated with increased neuronal responses. In the healthy SI of rats with forepaw denervation, increases in fMRI responses to forepaw stimulation are accompanied by increases in LFP amplitude and increased incidence of single unit responses compared with sham operated rats. In contrast, in the deprived SI, increases in fMRI responses are associated with minimal change in LFP amplitude and an increased incidence of single unit responses.

This discrepancy between increased fMRI responses and minimal LFP changes in the deprived cortex led to the characterization of the neuronal populations involved. Based on the AP duration, histology, and immunostaining results, the neurons showing increased responses to intact forepaw stimulation in the deprived cortex were identified as interneurons. These were most evident in laminae V and VI. In addition, some neurons identified by AP duration as pyramidal neurons in laminae V and VI of the deprived cortex showed significant decreases in firing rate during forepaw stimulation.

Through a complex cascade of neurovascular events, the BOLD response is tightly correlated to neuronal activity (7, 17, 18). Evidence shows that under normal conditions, BOLD response (7) and tissue oxygenation levels (19) are more correlated to synaptic activity than to spiking activity. In addition, decreases in cortical excitatory activity have been linked to decreases in BOLD signal (9, 10). Although information is growing about the signaling cascade that can induce vasoconstriction or vasodilatation and lead to a change in the BOLD signal [for review see Iadecola (20)], the exact relationship between specific types of neuronal activity, release of vasoactive substances, and the vascular response is still not quantitatively understood.

In the present study, we demonstrate that increased fMRI responses in the deprived cortex are specifically accompanied by increases in inhibitory interneuron activity and are unlikely due to increases in pyramidal neuronal activity. These results join a number of recent studies that have demonstrated brain regional increases in cortical blood flow that do not coincide with neuronal excitatory responses under specific stimulation paradigms. For example, increases in multiunit activity and glucose utilization have been correlated with decreased blood flow as measured with optical imaging techniques in rat ipsilateral SI after forepaw stimulation (21). Increases in blood flow in monkey visual cortex were not accompanied by increases in neuronal spiking activity during the period that the monkey was anticipating the onset of the actual trial (22) and decreases in BOLD responses in monkey visual cortex were not accompanied by changes in either spiking activity or high-frequency LFP power during perceptual suppression (23). Increased BOLD response in monkey SI after electrical stimulation of the median nerve was interpreted to reflect net local inhibition (14). In this study, the ipsilateral SI inhibition, measured with current source density analysis, was suggested to be mediated by intrahemispheric feedback inputs and not by transcallosal connections, demonstrating that increases in fMRI responses can reflect net inhibition in the intact cortex. In these cases, no specific classes of neurons were identified that might lead to the dissociation of blood flow and LFP detected. Only pharmacological manipulations of glutamate or GABA receptors (24, 25) have shown to cause dissociation of blood flow and LFP. Finally, there is precedent for plasticity-related response to loss of sensory input to cause an increase in inhibition in neuronal circuits. It was previously proposed that the increased inhibition in the visual cortex after visual deprivation can be mediated through either long-term depression of excitatory intracortical synapses (26) or potentiation of inhibitory synapses (27).

Previous results suggest that the transcallosal projections play a major role in the altered responses in the deprived SI because ablation of the healthy SI in the denervated rats eliminated the BOLD response in the deprived SI when the intact limb was stimulated (6). In rats, transcallosal projections specifically terminate in laminae II/III, V, and VI (28, 29). The neurons responding to ipsilateral, intact forepaw stimulation were found specifically in infragranular laminae and not in lamina IV, which receive the main thalamocortical input. In addition, firing rates of many pyramidal neurons in the infragranular laminae of the deprived cortex decreased during stimulation. These observations suggest that increases in firing responses in the deprived cortex are mediated through transcallosal connections. Both pyramidal neurons and interneurons receive direct callosal glutamatergic input from the contralateral homologous area (29). Therefore, denervation may alter the balance between inhibition and excitation in the deprived cortex so that pyramidal neurons are inhibited through a feed-forward mechanism from the surrounding interneurons that are also excited by the callosal input (29).

In summary, fMRI and electrophysiological measurements demonstrate that after a unilateral peripheral nerve injury, both the deprived and the healthy cortices undergo significant changes in their neuronal activity. The increased fMRI response in the deprived hemisphere is attributed to increased interneuron activity, probably mediated through callosal interhemi-

spheric projections. It remains to be determined how the increased activity in inhibitory interneurons in the deprived cortex influences the probability of recovery from nerve injury.

## Materials and Methods

All experiments were conducted in accordance with the National Institutes of Health *Guide for Care and Use of Laboratory Animals* and were approved by the National Institute of Neurological Disorders and Stroke Animal Care and Use Committee.

**Forepaw Denervation.** Denervation procedures were reported previously (6). Briefly, Sprague–Dawley rats (100 g, 5 weeks old; Harlan) underwent an excision of the forepaw radial, median, and ulnar nerves ($n = 25$). In the rat, these nerves contain sensory and motor fibers; thus, severing them removed both efferent and afferent components. All lesions were performed on the right forepaw. In control rats, the nerves were exposed as described, but were not cut (sham-operated, $n = 13$). Throughout the study, rats remained active and did not experience any significant weight loss or self-mutilation. Both fMRI and electrophysiology measurements took place 2–3 weeks after denervation.

**Functional MRI.** Seven denervated and seven sham-operated rats were initially anesthetized and maintained at 2% isoflurane during the surgical procedures for fMRI as described previously (6). Two needle electrodes were inserted just under the skin of each forepaw. After surgery, the rat was given an i.v. bolus of 80 mg/kg $\alpha$-chloralose (Sigma–Aldrich), and isoflurane was discontinued. Anesthesia was maintained with a constant $\alpha$-chloralose infusion (27 mg/kg/hr) and an i.v. injection of pancuronium bromide (4 mg/kg; AmerisourceBergen) was given once per hour to prevent motion. End-tidal $CO_2$, rectal temperature, tidal pressure of ventilation, heart rate, and arterial blood pressure were continuously monitored. Arterial blood gas levels were checked periodically, and corrections were made by adjusting respiratory volume or administering sodium bicarbonate. All images were acquired on an 11.7 T/31-cm horizontal bore magnet (Magnex Scientific), interfaced to an AVANCE console (Bruker BioSpin) and equipped with a 9-cm gradient set, capable of providing 64 G/cm with a rise time of 100 $\mu$s (Resonance Research). A linear birdcage coil (inner diameter of 69 mm) and a 12-mm-diameter surface coil transmitted and received signal, respectively. Scout images were acquired in three planes with a fast-spin echo sequence to determine appropriate positioning. A single-shot, gradient-echo, echo-planar imaging (EPI) sequence was run with the following parameters: effective echo time (TE) = 30 ms; repetition time (TR) = 750 ms; bandwidth = 200 kHz; field of view = 1.92 × 1.92 cm; 128 × 128 matrix size leading to a nominal in-plane resolution of 150 $\mu$m. Partial brain coverage was obtained with three, 1-mm-thick slices spaced 0.2 mm apart. A stimulator (World Precision Instruments) supplied 2.5-mA, 300-$\mu$s pulses repeated at 3 Hz to either the right or the left forepaw. The paradigm consisted of 10 dummy MRI scans to reach steady state, followed by 60 scans during rest and 15 scans during stimulation, which was repeated 4–5 times. The rat was allowed to rest between stimulation sets, and 3–5 sets of data were recorded from each rat for each forepaw.

**Electrophysiology.** Denervated ($n = 6$) or sham-operated rats ($n = 6$) were anesthetized with urethane (1.25 g/kg, i.p. initially with additional supplements as needed, Sigma–Aldrich) and were placed in a stereotaxic frame (Kopf Instruments). Craniotomies (0.5-mm square) were performed over the right and the left SI (anterior from bregma, 0 mm; lateral from midline, ±3.6 mm). A glass recording electrode (≈4-MΩ impedance (measured at 135 Hz) with tip diameter of 1–2 $\mu$m) filled with 2% Pontamine Sky blue dye in 2 M NaCl, was lowered to the target depth by using a micromanipulator (MO-8; Narishige International). Single-unit and LFP recordings were obtained. Starting at 50 $\mu$m below the cortical surface, LFP recordings were conducted every 150 $\mu$m until 1850 $\mu$m. When an action potential of a single neuron was identified, additional measurements of spike activity and LFP were performed. Thus, each recording track resulted in a minimum of 13 LFP measurements. For each denervated rat, data were obtained from a single track in the deprived cortex and a single track in the healthy cortex. For sham-operated rats, data were obtained from a single track from the SI ipsilateral to the sham-operated forepaw. Extracellular action potentials recordings were amplified (World Precision Instruments) and monitored on digital oscilloscopes (Hewlett-Packard) and audio monitors (Grass). Spikes and LFPs were band-pass filtered at 250–5,000 Hz and 0.1–100 Hz, respectively. Discriminated signals were collected with a CED interface and Spike2 data acquisition and analysis software (Cambridge Electronic Design). LFPs were sampled at 1,000 Hz and spikes at 25 KHz. Tactile stimulation was delivered through a Biopac system (BIOPAC Systems). The system supplied 2-mA, 300-$\mu$s pulses at 3 Hz to either the right or the left forepaws through two needle electrodes under the skin of each forepaw. Two hundred single stimuli (total time 66.6 s) were obtained for each measurement. In 10 rats, the last recording site was marked by iontophoresis of Pontamine blue dye from the recording electrode. Brains were sliced for verification of recording sites.

**In Vivo Juxtacellular Labeling.** Single neurons were labeled by using the technique of juxtacellular injection of neurobiotin (16) to identify morphological properties in an additional 12 denervated rats. Glass pipettes (15–20 MΩ at 135 Hz) were filled with 0.5 M NaCl and 2.0% neurobiotin (Vector Laboratories). Briefly, positive pulses of current (1–6 nA, 200-ms duration) were delivered at a frequency of 2.5 Hz through the bridge circuit of an Axoclamp 2A amplifier (Axon Instruments). The current was slowly increased, and the electrode was advanced by steps of ≈1 $\mu$m until the cell discharge was driven by the injected current. Current pulses were applied for a 10- to 15-min period to obtain reliable labeling of neuronal processes. An hour after neurobiotin injection, the animal was perfused as described previously (16). Brains were cut at 50 $\mu$m by using a freezing microtome. Neurobiotin was detected by incubation of the sections in the avidin–biotin peroxidase complex (1:100; Vector Laboratories) and then in a solution containing 0.05% 3,3′-diaminobenzidine tetrahydrochloride (Sigma–Aldrich). These sections were counterstained with Nissl. In other sections, streptavidin conjugated to Alexa Fluor 568 (Invitrogen) and monoclonal anti-parvalbumin [(Millipore) then detected with Alexa Fluor 488 anti-mouse IgG (Invitrogen)] were used to detect the neurobiotin- and paravalbumin-containing interneurons, respectively. Stained sections were imaged by using Zeiss 510 LSM inverted confocal microscope with ×40 objective.

**Data Analyses.** ***fMRI experiments.*** *Single-animal analysis.* Analysis of the fMRI time series for individual animals was performed by using STIMULATE (University of Minnesota, Minneapolis, MN). A correlation coefficient was calculated from cross-correlation of the unfiltered time series with a boxcar wave form representing the stimulation period. The activation threshold was set at 0.2, and the number of pixels above this threshold and their averaged amplitude in SI (15) were calculated for each dataset. The BOLD percentage change with standard deviation was obtained by calculating the average amplitude during the 5 stimulation epochs minus the average amplitude during rest and divided by the average amplitude during rest. A two-tailed unpaired Student's *t* test was performed between groups.

*Group analysis.* Group analysis was performed by custom-written software running in Matlab (The MathWorks) and a public domain tool for image registration (http://bishopw.loni.ucla.edu/AIR5/index). To facilitate within- and between-group comparisons and analysis, brain images of all animals were normalized to the same spatial dimension. By coregistering all of the EPI images to a brain template, variations in brain sizes and EPI distortions were reduced. Initially, a slice corresponding to the template images was chosen. To avoid the interference from the cortical lesions and skin, brain masks were created manually. The coregistration was performed in two steps by using automated image registration (AIR, version 5.2.5; http://bishopw.loni.ucla.edu/AIR5/index) to minimize the SD of ratios between two images (30). To reduce the gross differences in the brain positions, each image was coregistered to the template by a 2D rigid-body transformation. The differences in the brain size and distortion were considered in the second step by a 2D affine transformation, which incorporated scaling and shearing. Then the transformation was applied to all images, including different runs, from the same animal by using windowed sinc interpolation. To combine results from individual animals in the same group, the representative data from each animal were reanalyzed by a Student's *t* test:

$$t = \frac{\bar{x}_A - \bar{x}_R}{\sqrt{\hat{\sigma}^2(1/N_A + 1/N_R)}} \qquad \hat{\sigma} = \frac{(N_A - 1)\sigma_A^2 + (N_R - 1)\sigma_R^2}{(N_A + N_R - 2)} \qquad [1]$$

where $\bar{x}_i$, $\hat{\sigma}_i^2$, and $N_i$ are the mean intensity, variance, and number of time points, respectively, during activated (A) or resting (R) periods. A hemodynamic delay of one scan was used, and no spatial smoothing was applied to prevent degradation of the resolution. Then group *t*-score maps were created by using a fixed-effects analysis:

$$t = \frac{\bar{\hat{b}}}{\hat{\sigma}_{b\varepsilon}/\sqrt{N}} \qquad \bar{\hat{b}} = \frac{1}{N}\sum_{i=1}^{N}\hat{b}_i \qquad \hat{\sigma}_{b\varepsilon}^2 = \frac{1}{N}\sum_{i=1}^{N}\sigma_{b\varepsilon i}^2 \qquad [2]$$

where $\hat{b}_i$ is the mean signal change, i.e., the numerator in Eq. **1**, and $\sigma^2_{\hat{b}ei}$ is the common variance, i.e., the square of the denominator in Eq. **1**, of the *i*th animal, and *N* is the number of animals in that group. The group *t*-maps were threshold by $P < 10^{-4}$ (uncorrected for multiple comparisons). The within-subject reproducibility was checked by the same method for group analysis.

***Electrophysiology experiments.*** Analyses were performed by using Spike2 software. LFP waveforms were averaged with respect to the stimulation trigger (200 single stimulations) after removing the DC offset. The mean amplitude of the peak negative deflection and its delay after triggering were calculated for each train of stimuli. For group analysis, the amplitude and the delay of the peak negative deflection were averaged across rats at the same cortical depth. Spike sorting was conducted by using principal-component analysis. Post-stimulus time histograms were obtained for each neuron by event correlation analysis of the spiking with the stimulation by using 5-ms bins. For each neuron, the SD of spiking activity was calculated for the last 100 ms of the interstimulus interval. Neurons that showed increased (>2 SD) spiking in one 5-ms bin during the first 30 ms after the onset of the stimulation were considered to show stimulus-induced excitation (responding neurons). Baseline firing rate was calculated for a 50-s epoch before stimulation onset for all responding neurons. To quantify the response of those neurons that did not show excitatory activity to ipsilateral forepaw stimulation, firing rates during the last 50 s of the stimulation epoch and the first 50 s after stimulation termination were compared with baseline (the last 50 s before stimulation onset). Only those neurons that demonstrated at least 10% decrease or increase in firing rate were considered to be inhibited by the stimulation or to demonstrate rebound excitation, respectively. Measurement of AP duration was performed on the second phase of the spike wave form whether the wave form was triphasic or biphasic (Fig. 3*A*) (16). Results are shown as mean ± standard mean error.

**ACKNOWLEDGMENTS.** We thank Dr. Steve Dodd and Ms. Nadia Bouraoud for assistance. This work was supported by the Intramural Research Program of the National Institutes of Health, National Institute of Neurological Disorders and Stroke.

1. Dettmers C, et al. (2001) Increased excitability in the primary motor cortex and supplementary motor area in patients with phantom limb pain after upper limb amputation. *Neurosci Lett* 307(2):109–112.
2. Feydy A, et al. (2002) Longitudinal study of motor recovery after stroke: Recruitment and focusing of brain activation. *Stroke* 33(6):1610–1617.
3. Rocca MA, Filippi M (2007) Functional MRI in multiple sclerosis. *J Neuroimaging* 17 Suppl 1:36S–41S.
4. Duong TQ, Silva AC, Lee SP, Kim SG (2000) Functional MRI of calcium-dependent synaptic activity: Cross correlation with CBF and BOLD measurements. *Magn Reson Med* 43(3):383–392.
5. Hyder F, Behar KL, Martin MA, Blamire AM, Shulman RG (1994) Dynamic magnetic resonance imaging of the rat brain during forepaw stimulation. *J Cereb Blood Flow Metab* 14(4):649–655.
6. Pelled G, Chuang KH, Dodd SJ, Koretsky AP (2007) Functional MRI detection of bilateral cortical reorganization in the rodent brain following peripheral nerve deafferentation. *NeuroImage* 37(1):262–273.
7. Logothetis NK, Pauls J, Augath M, Trinath T, Oeltermann A (2001) Neurophysiological investigation of the basis of the fMRI signal. *Nature* 412(6843):150–157.
8. Devor A, et al. (2007) Suppressed neuronal activity and concurrent arteriolar vasoconstriction may explain negative blood oxygenation level-dependent signal. *J Neurosci* 27(16):4452–4459.
9. Ogawa S, et al. (2000) An approach to probe some neural systems interaction by functional MRI at neural time scale down to milliseconds. *Proc Natl Acad Sci USA* 97(20):11026–11031.
10. Shmuel A, Augath M, Oeltermann A, Logothetis NK (2006) Negative functional MRI response correlates with decreases in neuronal activity in monkey visual area V1. *Nat Neurosci* 9(4):569–577.
11. Lauritzen M (2001) Relationship of spikes, synaptic activity, and local changes of cerebral blood flow. *J Cereb Blood Flow Metab* 21(12):1367–1383.
12. Hamel E (2006) Perivascular nerves and the regulation of cerebrovascular tone. *J Appl Physiol* 100(3):1059–1064.
13. Cauli B, et al. (2004) Cortical GABA interneurons in neurovascular coupling: Relays for subcortical vasoactive pathways. *J Neurosci* 24(41):8940–8949.
14. Lipton ML, Fu KM, Branch CA, Schroeder CE (2006) Ipsilateral hand input to area 3b revealed by converging hemodynamic and electrophysiological analyses in macaque monkeys. *J Neurosci* 26(1):180–185.
15. Paxinos G, Watson C (1986) *The Rat Brain in Stereotaxic Coordinates* (Academic, Sydney), pp xxvi, [114] of plates.
16. Tierney PL, Degenetais E, Thierry AM, Glowinski J, Gioanni Y (2004) Influence of the hippocampus on interneurons of the rat prefrontal cortex. *Eur J Neurosci* 20(2):514–524.
17. Brinker G, et al. (1999) Simultaneous recording of evoked potentials and T2*-weighted MR images during somatosensory stimulation of rat. *Magn Reson Med* 41(3):469–473.
18. Duong TQ, Kim DS, Ugurbil K, Kim SG (2001) Localized cerebral blood flow response at submillimeter columnar resolution. *Proc Natl Acad Sci USA* 98(19):10904–10909.
19. Viswanathan A, Freeman RD (2007) Neurometabolic coupling in cerebral cortex reflects synaptic more than spiking activity. *Nat Neurosci* 10(10):1308–1312.
20. Iadecola C (2004) Neurovascular regulation in the normal brain and in Alzheimer's disease. *Nat Rev Neurosci* 5(5):347–360.
21. Devor A, et al. (2008) Stimulus-induced changes in blood flow and 2-deoxyglucose uptake dissociate in ipsilateral somatosensory cortex. *J Neurosci* 28(53):14347–14357.
22. Sirotin YB, Das A (2009) Anticipatory haemodynamic signals in sensory cortex not predicted by local neuronal activity. *Nature* 457(7228):475–479.
23. Maier A, et al. (2008) Divergence of fMRI and neural signals in V1 during perceptual suppression in the awake monkey. *Nat Neurosci* 11(10):1193–1200.
24. Gsell W, et al. (2006) Differential effects of NMDA and AMPA glutamate receptors on functional magnetic resonance imaging signals and evoked neuronal activity during forepaw stimulation of the rat. *J Neurosci* 26:8409–8416.
25. Caesar K, Thomsen K, Lauritzen M (2003) Dissociation of spikes, synaptic activity, and activity-dependent increments in rat cerebellar blood flow by tonic synaptic inhibition. *Proc Natl Acad Sci USA* 100(26):16000–16005.
26. Rittenhouse CD, Shouval HZ, Paradiso MA, Bear MF (1999) Monocular deprivation induces homosynaptic long-term depression in visual cortex. *Nature* 397(6717):347–350.
27. Maffei A, Nataraj K, Nelson SB, Turrigiano GG (2006) Potentiation of cortical inhibition by visual deprivation. *Nature* 443(7107):81–84.
28. Wise SP, Jones EG (1976) The organization and postnatal development of the commissural projection of the rat somatic sensory cortex. *J Comp Neurol* 168(3):313–343.
29. Karayannis T, Huerta-Ocampo I, Capogna M (2007) GABAergic and pyramidal neurons of deep cortical layers directly receive and differently integrate callosal input. *Cereb Cortex* 17:1213–1226.
30. Wood AK, Klide AM, Pickup S, Kundel HL (2001) Prolonged general anesthesia in MR studies of rats. *Acad Radiol* 8(11):1136–1140.